

Exciton dissociation and charge trapping at poly(3-hexylthiophene)/phenyl-C61-butyric acid methyl ester bulk heterojunction interfaces: Photo-induced threshold voltage shifts in organic field-effect transistors and solar cells

Byoungnam Park, Nam-Ho You, and Elsa Reichmanis

Citation: *J. Appl. Phys.* 111, 084908 (2012); doi: 10.1063/1.4705277

View online: <http://dx.doi.org/10.1063/1.4705277>

View Table of Contents: <http://jap.aip.org/resource/1/JAPIAU/v111/i8>

Published by the [American Institute of Physics](#).

Related Articles

The roles of metallic rectangular-grating and planar anodes in the photocarrier generation and transport of organic solar cells

[Appl. Phys. Lett.](#) 101, 223302 (2012)

The roles of metallic rectangular-grating and planar anodes in the photocarrier generation and transport of organic solar cells

[APL: Org. Electron. Photonics](#) 5, 255 (2012)

Towards the development of a virtual organic solar cell: An experimental and dynamic Monte Carlo study of the role of charge blocking layers and active layer thickness

[Appl. Phys. Lett.](#) 101, 193306 (2012)

Towards the development of a virtual organic solar cell: An experimental and dynamic Monte Carlo study of the role of charge blocking layers and active layer thickness

[APL: Org. Electron. Photonics](#) 5, 246 (2012)

Towards an understanding of light activation processes in titanium oxide based inverted organic solar cells

[J. Appl. Phys.](#) 112, 094503 (2012)

Additional information on *J. Appl. Phys.*

Journal Homepage: <http://jap.aip.org/>

Journal Information: http://jap.aip.org/about/about_the_journal

Top downloads: http://jap.aip.org/features/most_downloaded

Information for Authors: <http://jap.aip.org/authors>

ADVERTISEMENT



AIP Advances

Now Indexed in
Thomson Reuters
Databases

Explore AIP's open access journal:

- Rapid publication
- Article-level metrics
- Post-publication rating and commenting

Exciton dissociation and charge trapping at poly(3-hexylthiophene)/phenyl-C61-butyric acid methyl ester bulk heterojunction interfaces: Photo-induced threshold voltage shifts in organic field-effect transistors and solar cells

Byoungnam Park,¹ Nam-Ho You,² and Elsa Reichmanis^{1,3,4,a)}

¹*School of Chemical and Biomolecular Engineering, Georgia Institute of Technology, 311 Ferst Drive, N.W., Atlanta, Georgia 30332-0100, USA*

²*Institute of Advanced Composites Materials, Korea Institute of Science and Technology, 864-9 Dunsan-ri, Bongdong-eup, Wanju-gun, Jeollabuk-do 565-902, Korea*

³*School of Chemistry and Biochemistry, Georgia Institute of Technology, Atlanta, Georgia 30332-0100, USA*

⁴*School of Materials Science and Engineering, Georgia Institute of Technology, Atlanta, Georgia 30332-0100, USA*

(Received 2 January 2012; accepted 27 February 2012; published online 30 April 2012)

Photoinduced charge transfer at an electron donor/acceptor interface is one of the most crucial processes in determining the power conversion efficiency of organic solar cell devices. Here, we address exciton dissociation and charge carrier trapping at poly(3-hexylthiophene) (P3HT)/phenyl-C61-butyric acid methyl ester (PCBM) bulk heterojunction interfaces electrically using a field effect transistor (FET). With a P3HT/PCBM composite film, we elucidated exciton dissociation and charge carrier recombination assisted by localized electronic states at the P3HT/PCBM interface via photoinduced threshold voltage shift measurements with respect to wavelength using FETs in combination with organic solar cell devices. Interestingly, the combination of light coupled with a significant quantity of PCBM within the film was required to observe ambipolar charge transport in P3HT/PCBM FETs. This phenomenon was addressed by filling of electron traps associated with PCBM under illumination and formation of the conducting pathways for both electrons and holes. A high density of carrier traps at the interface suggested by the FET results was confirmed in light intensity dependent short-circuit current (J_{sc}) and open-circuit voltage (V_{oc}) measurements using solar cell devices. © 2012 American Institute of Physics. [<http://dx.doi.org/10.1063/1.4705277>]

I. INTRODUCTION

Molecular energy level alignment of the individual components at the organic/organic interface is an important consideration in the design and optimization of organic optoelectronic devices such as organic solar cells (OSCs), photo detectors and organic light emitting diodes (OLEDs).¹⁻⁴ Through appropriate choice of the constituents, efficient photoinduced charge transfer arising from optimized band offsets between an organic acceptor and donor can be achieved in OSCs, while the energy barriers between electron and hole transporting materials under forward bias conditions can be tuned for the confinement of electrons and holes to effect recombination in OLEDs.⁵

The key issue associated with optimization of organic device performance is the ability to probe the functional interfaces that have a crucial role in device operation. The electronic structures of the individual organic components comprising the interfaces are readily characterized by spectroscopic tools including ultraviolet photoelectron spectroscopy and x-ray photoelectron spectroscopy, and provide an estimate of the energy level offsets at the relevant interfaces.^{6,7} The information acquired relating to energy level

alignment between the organic components obtained by these spectroscopic methods is, however, not readily applied to designing the organic device structures since the interfacial electronic characteristics of the organic components are often significantly altered by the physical arrangement of the individual organic materials at the interface.^{8,9} For example, depending on molecular orientations of the organic components at the interface, an interface dipole can be induced in the film.⁹

Further, for OSCs, probing an electron donor/acceptor bulk heterojunction interface, which provides critical information for optimizing device performance, is challenging because exciton dissociation at the interface, buried within a thick composite film, competes with other processes including charge transport within the active layer and charge collection at electrodes. Here, in an effort to explore exciton dissociation at the interface and relevant electronic properties such as interfacial charge carrier traps eliminating other electronic processes in solar cell devices, we structured a bottom-contact field effect transistor (FET) using a model OSC system, namely, poly(3-hexylthiophene) (P3HT) as the electron donor and phenyl-C61-butyric acid methyl ester (PCBM) as the acceptor. Surprisingly, in the extensive work to enhance the power conversion efficiency of P3HT:PCBM bulk heterojunction solar cell devices, exciton dissociation

^{a)}Electronic mail: ereichmanis@chbe.gatech.edu.

and charge carrier trapping at the buried interface, excluding complications resulting from a stacked diode structure, has not been treated electrically using a combination of FET and solar cell structures, despite its huge implication.

A small drain voltage was applied to efficiently separate photogenerated carriers at the bulk heterojunction interface. Threshold voltage, which is the gate voltage required to observe mobile charge carriers in the conducting channel, reflects the number of charged states within a composite film resulting from exciton dissociation during illumination.¹⁰ The charge carrier density in the component materials of the composite film, modulated by the number of excitons dissociated at the P3HT/PCBM interface, changes the drain current I_d by changing the threshold voltage V_T , assuming that the FET mobility μ remains constant, as described in the Eq. (1),

$$I_d = \frac{Z}{L} \mu C_{oxide} (V_G - V_T) V_D, \quad (1)$$

where C_{oxide} is the capacitance per unit area of the silicon oxide gate dielectric, L is the channel length, and Z is the channel width. We characterized P3HT/PCBM composite films in the linear regime of transistor operation in which a small drain voltage V_D relative to the gate voltage V_G is applied.

II. EXPERIMENTAL SECTION

We constructed a FET device with a blend of P3HT and PCBM as the active layer. P3HT and PCBM were purchased from Sigma Aldrich and used without further purification. The P3HT had a M_n of 24 kD and M_w of 47.7 kD, as obtained from gel permeation chromatography (GPC) in tetrahydrofuran calibrated with polystyrene standards and a head to tail regioregularity of 92%–94%. The P3HT and PCBM solutions were prepared using chloroform as a solvent with the concentrations of 8 mg/mL and 14 mg/mL, respectively. Blends having different compositions of the two components were prepared by varying the weight ratio of the respective solutions. To serve as the conducting channel between source and drain electrodes (Au/Cr), two sets of P3HT/PCBM blends, P3HT:PCBM (1:15, w/w) and P3HT:PCBM (1:5, w/w), were spin-coated onto 200 nm thick SiO_2 gate dielectrics at 1500 rpm for 60 s, giving thicknesses of up to 210 nm. A highly doped silicon substrate was used as the gate electrode. For the threshold voltage measurement, a linear fit to the plot of drain current as a function of gate voltage was used to determine the extrapolated value on the gate voltage axis at $I_d = 0$. The current–voltage characteristic curves for the threshold voltage measurements, in the dark and under illumination in air, were obtained using a semiconductor parameter analyzer (HP4155B). Illumination with variable wavelengths (Figure 1) was performed using a grating monochromator (Optronic Laboratories, Inc. OL Series 750) with a 150 watt quartz-halogen light source in air. For the photoinduced threshold voltage measurements in which the light intensity is varied, two laser diodes with wavelengths of 520 and 620 nm were used to illuminate the samples and the intensity was measured with a power meter. Optical absorption spectra of P3HT and PCBM films were

obtained using a UV-Vis spectrometer. For fabrication of a P3HT/PCBM organic solar cell, films made from a blend of P3HT and PCBM solutions (1:15, w/w) in chloroform were prepared using spin-coating at 1500 rpm for 60 s onto a PEDOT:PSS/indium tin oxide (ITO) substrate. Al (~ 100 nm) was deposited onto the P3HT/PCBM active layer. All the electrical measurements were performed in air.

III. RESULTS AND DISCUSSION

A change in the threshold voltage shift can be correlated with a change in the electrostatic potential of the composite P3HT/PCBM film. Upon illumination, excitons within P3HT are dissociated at the interface, effecting electron transfer to PCBM, thus decreasing the electrostatic potential of the composite film. This process reduces the energy level difference ψ_B between the Fermi energy and the highest occupied molecular orbital (HOMO) of P3HT in the bulk. The threshold voltage can be expressed by the Eq. (2), assuming that the flat band voltage is zero^{11,12}

$$V_T = -\psi_B - \frac{\sqrt{2\varepsilon_s q N \psi_B}}{C_{oxide}}, \quad (2)$$

where ε_s is the dielectric constant of the semiconductor, q the elementary charge, N the doping concentration, and C_{oxide} the capacitance of the gate dielectric. The decrease in the value of ψ_B shifts the threshold voltage to a more positive value for hole conduction to take place. This model can also be adjusted to explain the threshold voltage shift for electron conduction in the PCBM component.

The threshold voltage shift observed under illumination for hole conduction in a FET fabricated with the P3HT/PCBM heterojunction interface was consistent with the optical absorption spectrum of P3HT. Threshold voltage shifts for a FET device prepared with the composite film were observed under illumination with wavelengths between 500 and 900 nm, as shown in Figures 1(a) and 1(b). The inset in Figure 1(a) shows the bottom contact FET configuration used in these experiments. To measure the threshold voltage for p -channel conduction, the gate voltage was swept from 20 to -60 V with a drain voltage of -5 V in Figure 1(a). The value of the threshold voltage measured in the dark was 4 V, and the change observed when the device was illuminated with wavelengths between 700 and 900 nm was less than 3 V. A relatively large threshold voltage shift of 9 V was observed for illumination with a wavelength of 500 nm at an intensity of $30 \mu\text{W}/\text{cm}^2$, where the optical absorption of P3HT is strong.^{13,14} The values of the threshold voltage shift obtained from Figure 1(a) were normalized to the incident photon flux in the scanned wavelength range. Figure 1(b) shows a plot of the normalized threshold voltage shift per unit incident photon as a function of wavelength. The relatively small threshold voltage shift observed for wavelengths over 700 nm and the large shift occurring at roughly 500 nm coincides with the UV-Vis absorption spectroscopic data for P3HT, as shown in Figure 1(c). These results support the premise that the threshold voltage shift observed in

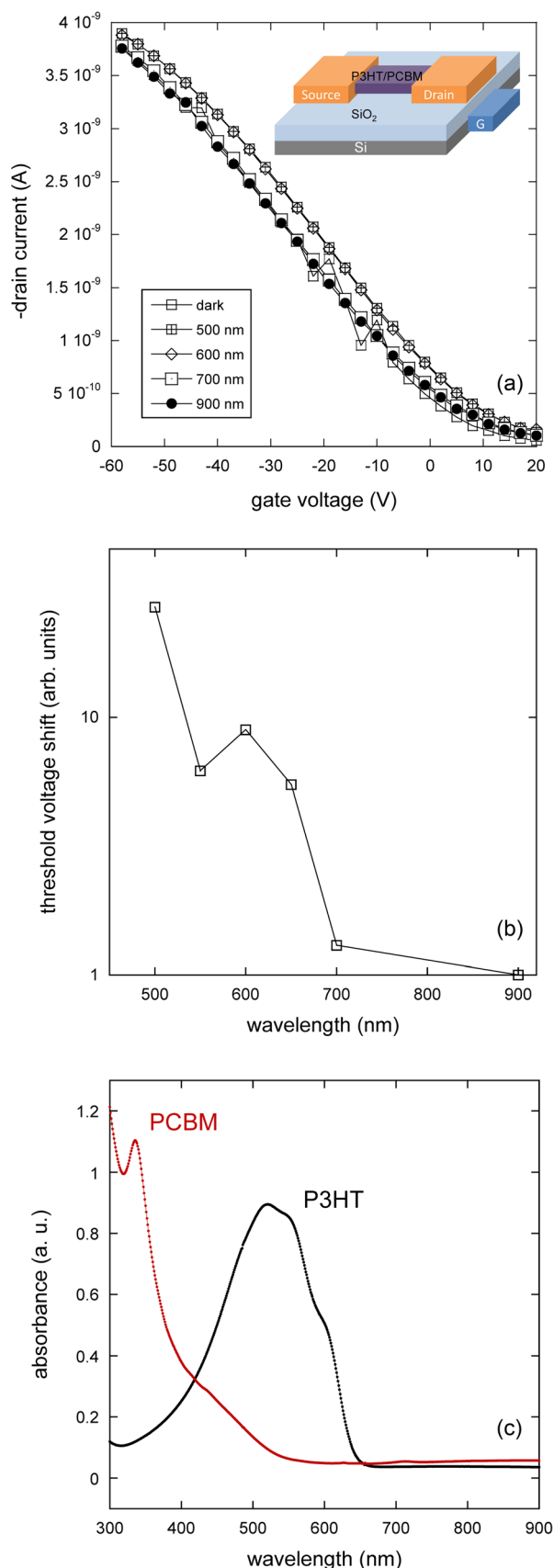
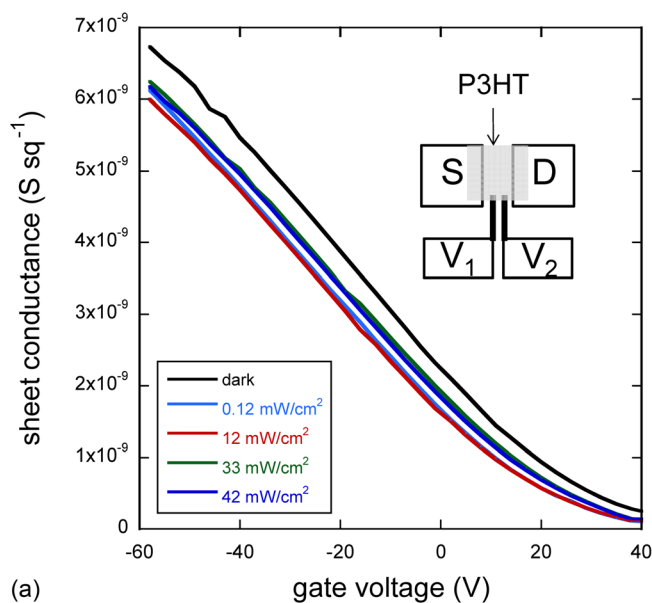


FIG. 1. (a) Plot of drain current vs. gate voltage for a FET fabricated with a P3HT:PCBM (1:15, w/w) bulk heterojunction interface. The inset shows a schematic diagram of the bottom-contact FET configuration used in the experiments. (b) Plot of normalized threshold voltage shift to the incident number of photons as a function of wavelength. (c) Optical absorption spectra of P3HT and PCBM.

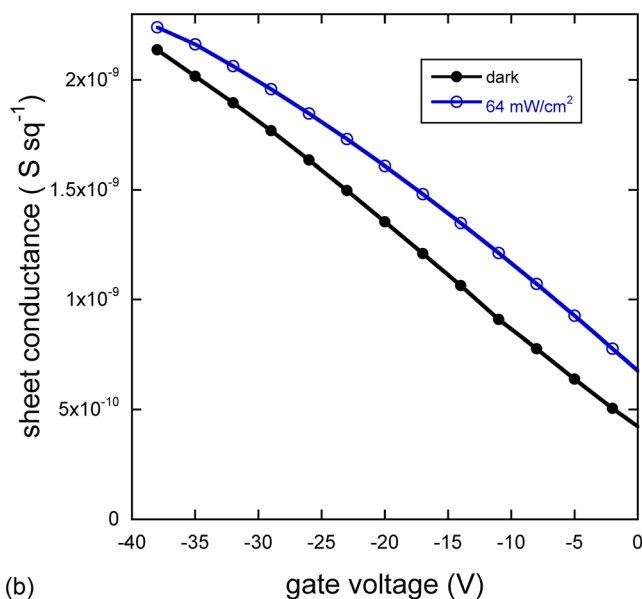
P3HT mainly arose from exciton dissociation at the P3HT/PCBM interface, leaving holes in the P3HT component.

To ensure the role of PCBM as the layer that accumulates electrons during illumination in changing the magnitude of the threshold voltage, pure P3HT was used in the same device configuration to measure threshold voltage under illumination. In the experiment, a four-point field effect device was used to exclude P3HT/Au contact resistance.¹⁵ This experiment was performed because it has been reported that the threshold voltage for a FET can be altered by a change in the charge injection barrier at the metal-semiconductor interface.¹⁶ Two four-point gated devices (see the inset) prepared with parent P3HT films were illuminated with red (620 nm) and green (520 nm) laser diodes and varying light intensities as shown in Figures 2(a) and 2(b). The threshold voltage observed for the P3HT FET in the dark was 27 V, a value which is comparable with literature reports for P3HT FETs measured in air.^{17,18} With a rise in the light intensity to 0.12 mW/cm² as seen in Figure 2(a), the threshold voltage shifted to a more negative value, 22 V, a direction opposite to that observed for the FETs prepared with P3HT/PCBM composite films. A further increase in the light intensity to 42 mW/cm² resulted in no further change in the value of the threshold voltage and only a slightly lower sheet conductance than that in the dark was noted, indicating that the contribution of photogenerated carriers in P3HT in enhancing the hole conductivity is not significant. When illuminated with green light (520 nm) with an intensity of 64 mW/cm² in Figure 2(b), the threshold voltage of the P3HT devices shifted by 3 V to a more positive value with a slightly larger sheet conductance at the full scan range of the gate voltage due to enhanced photoconductivity. This result is consistent with the strong optical absorption associated with P3HT in the wavelength range of 500 nm, as observed in Figure 1(c). More importantly, the magnitude of the shift was very small when compared to the shift of 36 V obtained with a FET fabricated with a P3HT/PCBM composite film at the same light intensity (Figure 3). In the absence of PCBM, the electrostatic potential change in the P3HT film is negligible due to significant recombination loss of photogenerated carriers, supported by a small increase in the sheet conductance resulting from a short carrier life time in the conducting channel upon illumination.

The threshold voltage shift observed under illumination is influenced by the electronic states at the P3HT/PCBM interface as well as exciton dissociation. In particular, the presence of localized electronic states at the P3HT/PCBM interface can increase the threshold voltage for electron conduction in PCBM because mobile electrons in the PCBM acceptor are available after filling the deep traps present at the interface. In a FET prepared with a P3HT/PCBM composite film, no electron transport was observed upon illumination under low intensity (0.12 mW/cm²) conditions with a gate scan from 60 to -10 V, as shown in Figure 3. Upon increasing the light intensity to 12 mW/cm², ambipolar charge transport was observed in the FET indicating that in the dark, the lack of electron current is not because the electron conducting path is incomplete, but rather, the threshold voltage for electron conduction has not yet been achieved in



(a)



(b)

FIG. 2. Plot of sheet conductance as a function of gate voltage for P3HT FETs in the dark and under illumination using laser diodes with wavelengths of (a) 620 nm and (b) 520 nm in the linear regime of transistor operation. The inset shows a schematic diagram of a four-point field-effect device with two voltage probes V_1 and V_2 , spaced by $30 \mu\text{m}$. The channel length between the source (S) and drain (D) electrodes was $80 \mu\text{m}$ and the thickness of the P3HT film was $\sim 30 \text{ nm}$.

the gate voltage range scanned. When the light intensity increased from 12 to 33 mW/cm^2 , a 7 V threshold voltage shift, from 19 to 12 V, was observed. For a control sample prepared using PCBM in the absence of P3HT, the threshold voltage in the dark was 20 V. Under illumination at a comparable light intensity to that used for the blended system, and the threshold voltage underwent a 3 V shift to a more positive value (from 20 to 23 V), a change that is attributed to the absence of the electron donor, P3HT. The large positive threshold voltage, at least more than $\sim 80 \text{ V}$, for electron conduction in the composite film, is suggested to be associated with a high density of electron traps at the P3HT/PCBM interface. Upon illumination, electrons transferred to PCBM

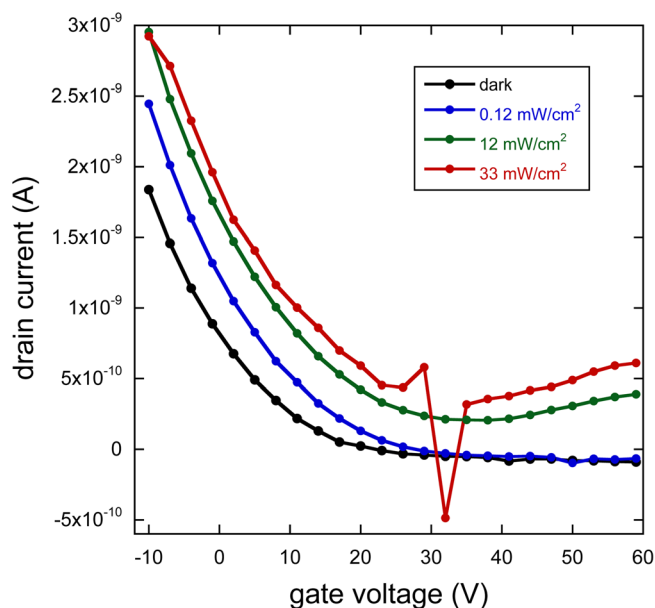


FIG. 3. Plot of drain current as a function of gate voltage for a FET fabricated with P3HT/PCBM (1:15, w/w). The drain voltage was fixed at 5 V.

from P3HT can fill deep traps associated with PCBM, thereby shifting the threshold voltage in the negative direction.

The presence of a high density of electron traps at the P3HT/PCBM interface can be addressed by light intensity dependent photocurrent measurements, useful in elucidating recombination loss of dissociated carriers at donor/acceptor interfaces in organic solar cells made with bulk heterojunction interfaces.^{1,19,20} Organic solar cells with P3HT/PCBM bulk heterojunction interfaces were fabricated as shown in the inset of Figure 4(a). In Figure 4(a), the short circuit current J_{sc} and open-circuit voltage V_{oc} were measured with increasing light intensity. In the intensity range of 30 to 130 mW/cm^2 , fitting of the power law, $J_{sc} \propto G^\alpha$, produces $\alpha = 0.56$ [Figure 4(b)]. Powers less than unity have been attributed to space charge effects^{21,22} due to unbalanced charge transport for electrons and holes or bimolecular recombination^{23,24} at donor/acceptor bulk heterojunction interfaces. If we assume that the value of $\alpha = 0.56$ originates from recombination limited carrier loss, justified by the fact that $\alpha = 0.75$ in the presence of space charge limited photocurrent,²² V_{oc} dependence on light intensity G can provide insights into possible recombination mechanisms. With Langevin recombination (bimolecular recombination) being dominant, V_{oc} can be expressed by Eq. (3),²⁵

$$V_{oc} = \frac{E_{gap}}{q} - \frac{kT}{q} \ln \left[\frac{(1-P)\gamma N_c^2}{PG} \right], \quad (3)$$

where E_{gap} is the energy level difference between the lowest unoccupied molecular orbital (LUMO) of the electron acceptor (PCBM) and the HOMO of the electron donor (P3HT), q is the elementary charge, k is the Boltzmann constant, T is the temperature, P is the exciton dissociation probability, γ is the recombination constant, N_c is the effective density of states in the conduction band, and G is the exciton generation rate.

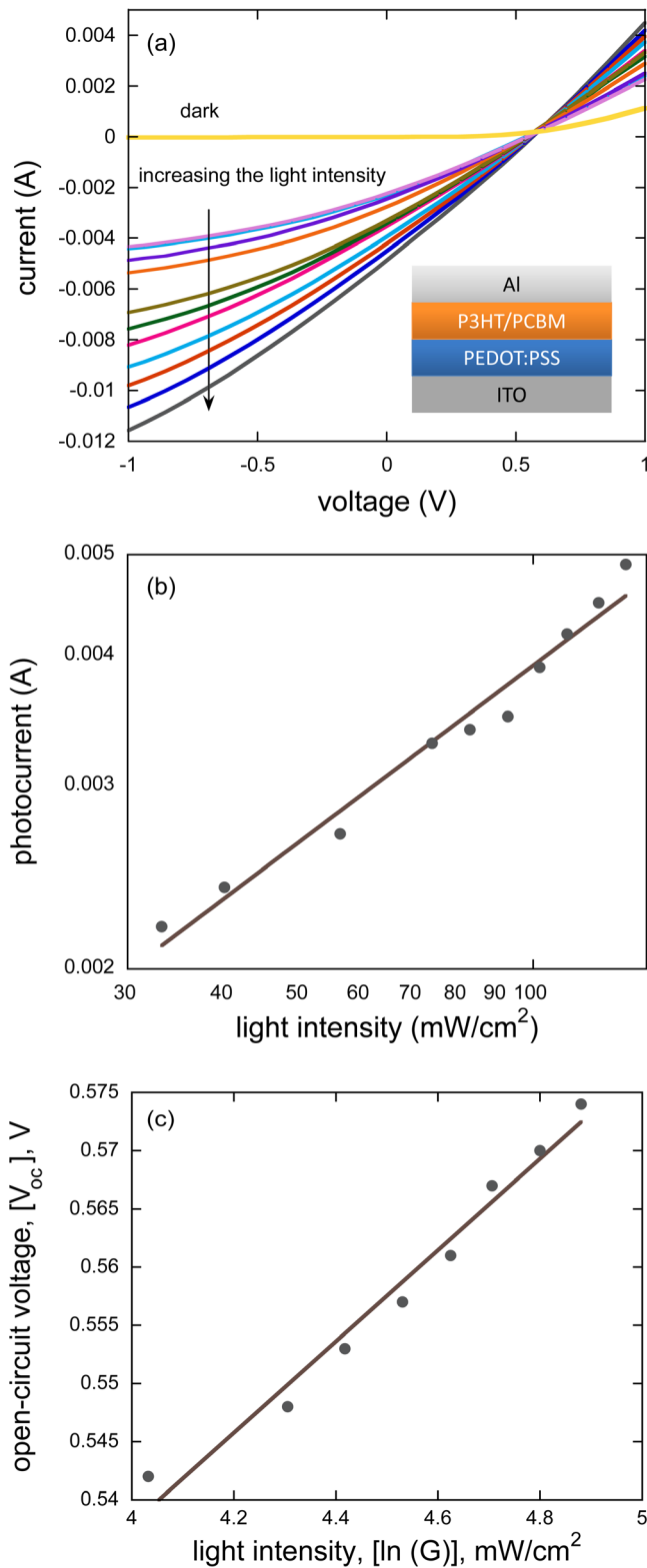


FIG. 4. (a) Current-voltage characteristic curves for a P3HT/PCBM (1:15, w/w) solar cell in the dark and under illumination. The inset shows a schematic diagram of a P3HT/PCBM bulk heterojunction solar cell device. (b) Plot of photocurrent as a function of light intensity. (c) Plot of open-circuit voltage as a function of light intensity.

According to the expression, the slope in the plot of V_{oc} vs. $\ln G$ is kT/q . In our solar cell device, the slope in Figure 4(c) is $1.5(kT/q)$. The deviation from kT/q has previously been explained by the competition between trap-assisted recombina-

tion (monomolecular recombination) and bimolecular recombination.^{26,27} The addition of the monomolecular recombination mechanism is suggested to be due to a high density of electron traps at the P3HT/PCBM interface, a supposition supported by the far larger positive threshold voltage for electron conduction within PCBM in the P3HT/PCBM FETs in comparison with that in pure PCBM FETs. Further, we measured the light intensity dependent threshold voltage shift using P3HT/PCBM FETs (Figure 5). The threshold voltage, proportional to the photocurrent in P3HT based on the assumption that the FET hole mobility remains constant both in the dark and under illumination, increased with increasing light intensity. In the low intensity regime below 10 mW/cm^2 , the fitting of $V_T \propto G^\alpha$ (see the inset) afforded $\alpha = 0.35$, and with increasing light intensity the value decreased to 0.25. The observed decrease in α may reflect the possibility that a significant number of electrons trapped in PCBM increased the built in electric field, preventing further electron transfer to PCBM. The origin of the lower value of α obtained from the P3HT/PCBM FET measurements in comparison with that from the solar cell device is not clear. However, the different bias conditions and active layer geometry between FET and solar cell devices may provide an explanation.

To observe ambipolar charge transport in a FET with P3HT/PCBM as the active layer, the formation of conducting pathways for both carriers between electrodes is essential. Therefore, information of the threshold voltage shift for electron and hole conduction in a FET device with an electron acceptor/donor interface can provide insights into the interfacial morphology. In the P3HT/PCBM bulk heterojunction interface, a significant fraction of PCBM in the composite film was required for electron conduction to be observed, as summarized in Table I. For both compositions evaluated here and measured in the dark, no electron conduction was observed with a gate voltage in the range -50 to 100 V. During illumination, however, the threshold voltage shift for

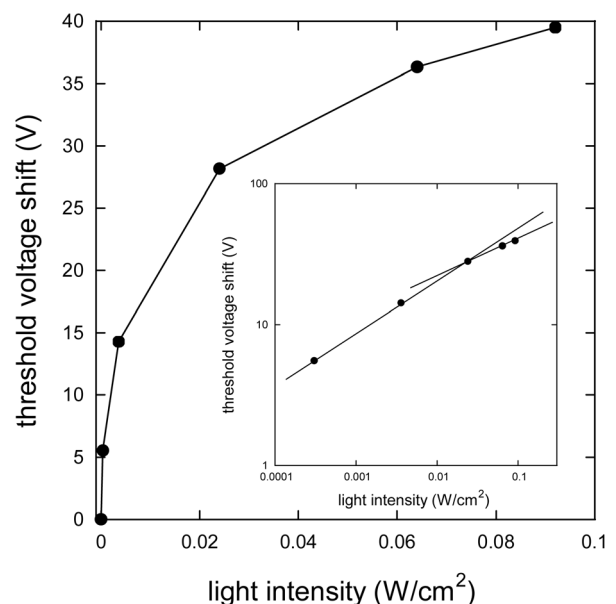


FIG. 5. Dependence of threshold voltage for hole conduction on light intensity (520 nm) for a P3HT/PCBM FET. The inset shows the plot of threshold voltage as a function of light intensity on a logarithmic scale.

TABLE I. Summary of the threshold voltage values in the dark and under illumination for FETs fabricated with two different P3HT/PCBM compositions.

		P3HT:PCBM = 1:15 (w/w)	P3HT:PCBM = 1:5 (w/w)
Dark	$V_{T,\text{hole}}$ (V)	19	19
	$V_{T,\text{electron}}$ (V)	No electron conduction	No electron conduction
620 nm	$V_{T,\text{hole}}$ (V)	30	20
	$V_{T,\text{electron}}$ (V)	11	No electron conduction
520 nm	$V_{T,\text{hole}}$ (V)	36	33
	$V_{T,\text{electron}}$ (V)	-120	No electron conduction

electron conduction was significant for a P3HT/PCBM composite film, having a weight ratio of 1:15, with values of more than 90 V for illumination at 620 nm and 220 V for illumination at 520 nm. The magnitude of the photoinduced threshold voltage shift for electron conduction may be overestimated since it was difficult to define a linear fit in the transfer characteristic plot due to the very low electron current on the level of hundreds of pico-amperes. For the composite film prepared with much less PCBM (P3HT:PCBM = 1:5, w/w), no electron current was observed either in the dark or under illumination. This effect can be attributed to incomplete formation of the conducting pathways for electron transport in PCBM for this composition. Within a P3HT/PCBM composite film, PCBM is thought to be dispersed among P3HT molecular chains, consistent with the description suggested by Erb *et al.*²⁸ Formation of the conducting channel for hole transport in the P3HT is expected to be more favorable than in PCBM because the long P3HT chains span far larger areas than the clustered PCBM molecule, a representation which is consistent with our results. However, our FET geometry which is distinctly different from a solar cell device consisting of stacked layers should be considered in interpreting the observations. For example, the morphology of the composite film near a SiO₂ gate dielectric may differ from the morphology of the bulk since the surface energy of SiO₂ can influence film formation. This may lead to apparent inconsistencies in results obtained from solar cell and FET device architectures because structural properties of the composite film near the gate dielectric governs the electrical properties of the FET. Further, hydroxyl groups on the surface of a gate dielectric are known to function as electron trapping sites,²⁹ reducing the magnitude of the drain current significantly. Electron traps associated with oxygen molecules in PCBM can be created upon exposure to air, limiting detection of conducting channel formation through threshold voltage measurements. Indeed, earlier studies^{30,31} of P3HT/PCBM solar cells have shown that a weight ratio of about 1:1 affords the best solar cell performance, and is reflective of the difference in geometry of FETs and solar cells. Therefore, to validate our proposed strategy to probe electron donor/acceptor interfaces, surface treatment of the gate dielectric in a controlled environment would be desirable for future studies.

IV. SUMMARY AND CONCLUSION

In conclusion, we demonstrated that the threshold voltage measured in a FET configuration is an effective probe of

exciton dissociation at electron donor/acceptor interfaces, providing essential information concerning localized electronic states at the interface as well as the formation of conducting pathways within an electron donor/acceptor composite film. This strategy can be expanded to facilitate identification of the optimum composition of an electron donor/acceptor composite film that provides for balanced electron and hole transport, minimizing trap density at the interface via proper choice of materials. It is found that charge carrier traps are induced in the film upon formation of the bulk heterojunction interface, thereby changing the threshold voltage. When attempting to enhance solar cell performance through interface modification or thermal annealing, these charge carrier traps present at the interface must be taken into account. Structuring an electron donor/acceptor bulk heterojunction interface in a FET device can assist not only in the investigation of photoinduced charge transfer at the interface, but also in probing the carrier traps electrically, allowing for a systemic approach to optimizing OSCs. The information acquired through this methodology may also be used for the determination of the best combination of donor/acceptor components for the active layers of devices such as OSCs and photo detectors.

ACKNOWLEDGMENTS

This research was funded in part by the Center for Organic Photonics and Electronics (COPE), Georgia Tech, the CMDITR STC Program of the National Science Foundation (DMR-0120967), and the Korea Institute of Science and Technology (KIST) Institutional program.

¹R. A. J. Janssen, J. C. Hummelen, and N. S. Saricifti, *MRS Bull.* **30**(1), 33 (2005).

²C. J. Brabec, N. S. Saricifti, and J. C. Hummelen, *Adv. Funct. Mater.* **11**(1), 15 (2001).

³J. Shinar and R. Shinar, *J. Phys. D: Appl. Phys.* **41**(13), 133001 (2008).

⁴J. J. M. Halls, C. A. Walsh, N. C. Greenham, E. A. Marseglia, R. H. Friend, S. C. Moratti, and A. B. Holmes, *Nature (London)* **376**(6540), 498 (1995).

⁵H. Becker, S. E. Burns, and R. H. Friend, *Phys. Rev. B* **56**(4), 1893 (1997).

⁶W. Y. Gao and A. Kahn, *Appl. Phys. Lett.* **79**(24), 4040 (2001).

⁷O. V. Molodtsova and M. Knupfer, *J. Appl. Phys.* **99**(5), 053074 (2006).

⁸N. Koch, I. Salzmann, R. L. Johnson, J. Pflaum, R. Friedlein, and J. P. Rabe, *Org. Electron.* **7**(6), 537 (2006).

⁹H. Yamane, Y. Yabuuchi, H. Fukagawa, S. Kera, K. K. Okudaira, and N. Ueno, *J. Appl. Phys.* **99**(9), 093706 (2006).

¹⁰F. Yan, J. H. Li, and S. M. Mok, *J. Appl. Phys.* **106**(7), 074501 (2009).

¹¹T. B. Singh, R. Koeppel, N. S. Saricifti, M. Morano, and C. J. Brabec, *Adv. Funct. Mater.* **19**(5), 789 (2009).

¹²S. Scheinert and G. Paasch, *Phys. Status Solidi A* **201**(6), 1263 (2004).

- ¹³P. E. Shaw, A. Ruseckas, and I. D. W. Samuel, *Adv. Mater.* **20**(18), 3516 (2008).
- ¹⁴M. Shibao, T. Morita, W. Takashima, and K. Kaneto, *Thin Solid Films* **516**(9), 2607 (2008).
- ¹⁵B. Park, A. Aiyar, J. I. Hong, and E. Reichmanis, *ACS Appl. Mater. Interfaces* **3**(5), 1574 (2011).
- ¹⁶C. S. S. Sangeeth, P. Stadler, S. Schaur, N. S. Sariciftci, and R. Menon, *J. Appl. Phys.* **108**(11), 113703 (2010).
- ¹⁷A. M. Song, Y. M. Sun, X. F. Lu, S. W. Lin, J. Kettle, and S. G. Yeates, *Org. Electron.* **11**(2), 351 (2010).
- ¹⁸Y. R. Liu, L. M. Wu, P. T. Lai, and Q. Y. Zuo, *Semicond. Sci. Technol.* **24**(9), 095013 (2009).
- ¹⁹T. M. Clarke and J. R. Durrant, *Chem. Rev.* **110**(11), 6736 (2010).
- ²⁰S. R. Cowan, A. Roy, and A. J. Heeger, *Phys. Rev. B* **82**(24), 245207 (2010).
- ²¹L. J. A. Koster, V. D. Mihailetchi, H. Xie, and P. W. M. Blom, *Appl. Phys. Lett.* **87**(20), 203502 (2005).
- ²²V. D. Mihailetchi, J. Wildeman, and P. W. M. Blom, *Phys. Rev. Lett.* **94**(12), 126602 (2005).
- ²³P. Schilinsky, C. Waldauf, and C. J. Brabec, *Appl. Phys. Lett.* **81**(20), 3885 (2002).
- ²⁴I. Riedel, J. Parisi, V. Dyakonov, L. Lutsen, D. Vanderzande, and J. C. Hummelen, *Adv. Funct. Mater.* **14**(1), 38 (2004).
- ²⁵L. J. A. Koster, V. D. Mihailetchi, R. Ramaker, and P. W. M. Blom, *Appl. Phys. Lett.* **86**(12), 123509 (2005).
- ²⁶M. M. Mandoc, F. B. Kooistra, J. C. Hummelen, B. de Boer, and P. W. M. Blom, *Appl. Phys. Lett.* **91**(26), 263505 (2007).
- ²⁷M. M. Mandoc, W. Veurman, L. J. A. Koster, B. de Boer, and P. W. M. Blom, *Adv. Funct. Mater.* **17**(13), 2167 (2007).
- ²⁸T. Erb, U. Zhokhavets, G. Gobsch, S. Raleva, B. Stuhn, P. Schilinsky, C. Waldauf, and C. J. Brabec, *Adv. Funct. Mater.* **15**(7), 1193 (2005).
- ²⁹L. L. Chua, J. Zaumseil, J. F. Chang, E. C. W. Ou, P. K. H. Ho, H. Sirringhaus, and R. H. Friend, *Nature (London)* **434**(7030), 194 (2005).
- ³⁰W. L. Ma, C. Y. Yang, X. Gong, K. Lee, and A. J. Heeger, *Adv. Funct. Mater.* **15**(10), 1617 (2005).
- ³¹G. Li, V. Shrotriya, J. S. Huang, Y. Yao, T. Moriarty, K. Emery, and Y. Yang, *Nature Mater.* **4**(11), 864 (2005).